POLITECNICO MILANO 1863

SCUOLA DI INGEGNERIA INDUSTRIALE E DELL'INFORMAZIONE

Executive Summary of the Thesis

Characterization of an air lubrication system inspired by penguins

Laurea Magistrale in Mechanical Engineering - Ingegneria Meccanica

Author: Konstantinos Georgoussis

Advisor: Prof. Giovanni Bianchi

Co-advisor: Prof. Simone Cinquemani

Academic year: 2025-2026

1. Introduction

Energy efficiency is one of the main problems of modern day, this is because it is directly linked to emissions and global warming. A big sector where efficiency could be improved is aquatic transportation. This thesis focuses on developing a system inspired by the penguin that can generate bubbles to reduce drag in water. This system is inspired by penguins and especially their feathers, which can store air and release it into very fine bubbles when they want to accelerate. Also, research on the parameters that influence bubble size was implemented. Then, the test bench design and the building process are introduced, which will be used to move the vessels in the pool. Two vessels were designed, one inspired by the penguin and one with a torpedo shape, to understand whether this beneficial effect is dependent on the penguin shape or can be translated to objects of any shape. A system dedicated to generating bubbles has been developed for each vessel, and they were tested in a dedicated test bench.

2. Bubble drag reduction in penguins and applications

2.1. The plumage of the penguin

According to Williams et al. [4], the emperor penguin's feathers can be grouped into four main categories: contour feathers, afterfeathers, plumules, and filoplumes, based on their role. Examples can be seen in Figure 1. The contour feathers are the stiff outer layer of body feathers that protect the bird's skin. They provide a rigid and impenetrable waterproof cover over a thick, insulative layer. Afterfeathers and plumules are both soft, downy feathers that make up the insulation component of many avian species' plumage. Afterfeathers are attached to contour feathers, while plumules are separate feathers that attach directly to the skin. Lastly, filoplumes are very small feather structures consisting of a long, bare rachis (shaft) with short barbs and barbules only at the very tip of the rachis.

Figure 1: Photograph of a Pygoscelis papua penguin plumage, showing the overlapping layered structure of its body feathers.[5]

The barbs of the feathers tend to mix up, making an interwoven mesh (Figure 1) that is tightly packed, multilayered, and can be simulated as a porous material. These pore sizes can be approximated to be less than 20 μm [1]. The porous mesh created from the plumage holds air. When they dive with erected feathers, there is room for an air layer about 25 mm thick. They subsequently dive to 15 to 20 m, at which depth the air volume will have decreased by a substantial amount. During the dive, or when achieving that depth, they depress the feathers to fix the plumage volume at the new, decreased level. When the birds swim quickly upwards, the decompressing air will flow out by virtue of the available fixed plumage volume being substantially less than the initial volume.

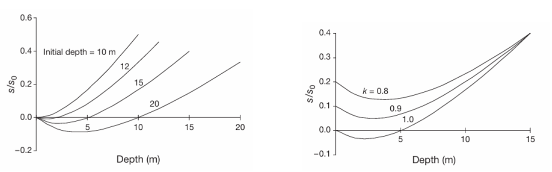

(a) (b)

Figure 2: Air layer thick ness (s/s_0) versus depth (d, in m) during ascent with constant velocity (V = 5.3 m/s) and constant air release, showing the effect of increasing initial depth (a), and showing the effect of decreasing entrapped air used up k (b).[1]

The Figure 2 shows the reduction of the air layer as the penguin ascends as a function of initial depth d_0, ascending speed V, and percentage of used air k.[1]

2.2. Air bubble characteristics

A formula given by [2] shows the effect of cross-flow velocity since the bubble diameter is directly disproportional with the velocity of the cross-stream, and proportional with the speed of the air that is exiting the orifice. Also, the relation with the opening of the orifice is visible. Since the bubbles were non-spherical, the bubble radius was determined as that of the volume equivalent sphere. The following statistical correlation was obtained for bubble departure radius in the single-bubble regime, explaining the data within ± 10%.

$$R_b = 0.48\, R_o^{0.826} \left(\frac{U_{gi}}{U_L} \right)^{0.36} \quad (1)$$

where:

- R_b is the volume-equivalent bubble departure radius,
- R_o is the orifice radius,
- U_{gi} is the superficial orifice gas velocity,
- U_L is the mean liquid cross-flow velocity.

These equations refer to bubbles exiting from orifices. Penguin feathers are a more complex geometry of an interwoven mesh, but we can simulate it as a porous material with pores the size of 20 μm. With this assumption, and a penguin able to reach a maximum speed of 5.3 m/s [1], as well as an air outflow velocity of 0.008 m/s. The equation (1) calculates an average bubble radius of 3.43 μm. Which is in line with the literature of very fine bubbles.

2.3. State of the art

A robotic penguin was developed by Pan et al. [3] that was able to swim forward by using its 2 wings, Figure 3.

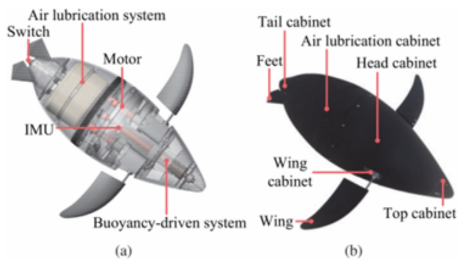

Figure 3: Illustration of the robotic penguin. (a) Conceptual design. (b) Robotic prototype.[3]

The Air Lubrication System (ALS) of the robotic penguin is designed to generate stable microbubbles around the hull to reduce skin friction. It consists of a 3 MPa compressed gas cylinder, a microcontroller-actuated solenoid valve, and a cabinet shell with 1 mm inclined holes positioned near the robot's largest cross-section to maximize bubble coverage. Testing was performed with the ALS closed and open, and results were recorded for the maximum speed the robot achieved. The results are shown below.

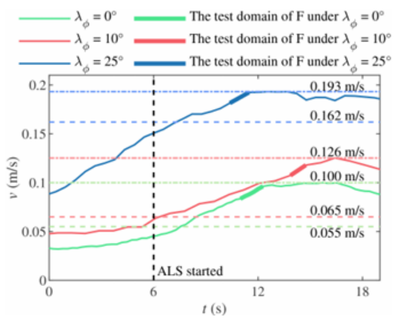

Figure 4: Experimental results of the forward speed for different wing angles with air lubrication (ALS). [3]

It is clearly observed (Figure 4) that when the ALS is turned on, there is a significant increase in the speed of the penguin, verifying the hypothesis that bubbles can reduce drag in water.

3. Test bench design

The concept idea for the testing bench is a 2-tower structure, one along each side of the pool, that are linked with 2 cables, along which a cart or sled is pulled. The pull motion will be performed with the help of a pulley system and a motor.

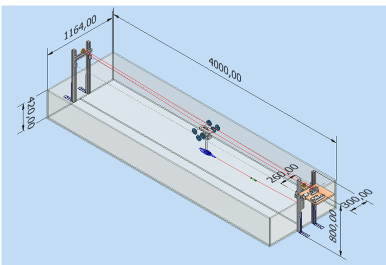

Figure 5: CAD of the test bench.

The body is going to be positioned underwater with the help of some threaded bolts and nuts, that connect it to the sled. The sled can move only on the cables in their direction, which stabilizes the system and prevents it from moving in different directions. Lastly, the load cell is attached to the robot directly.
As shown in Figure 5, the motor and the drum pull both the sled and the penguin robot using ropes and a pulley system. This is done in order to eliminate any friction reading from the load cell. Since the penguin robot is not fixed to the sled but just resting below it, the system is decoupled. Meaning that there is relevant movement between the robot and the sled. So the reading of the sensor is as clean as possible. The sled was designed using wheels to grip the cables to reduce the drag that the system was experiencing, as shown in Figure 6.

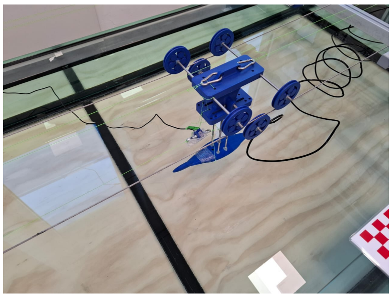

Figure 6: The experimental setup.

For the system to be able to run, electrical components were introduced. These involve a motor, a motor drive, a potentiometer, an Arduino Due, and a power supply. The motor that was used is a DC motor (24V, 3500 rpm) that was deemed sufficient to pull the sled. As a motor drive, the L298N board was picked. The diagram of the connection can be seen in the Figure 7 below.

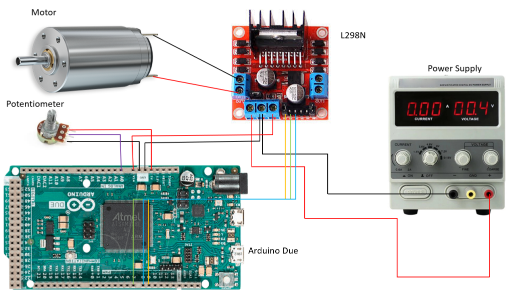

Figure 7: Schematic diagram of the connections of the system.

4. Modeling of the prototypes

4.1. Penguin Inspired vessel

To examine the effects of bubbles on underwater bodies, a body was designed that drew inspiration from the penguin. Penguins, unlike most underwater vehicles used today, are not cylindrical but have an elliptical profile. So the idea was to design an underwater vehicle that mimics this shape. The CAD design that was produced is shown in Figure 8. The hole design was created using a 3D printer and PETG as the material.

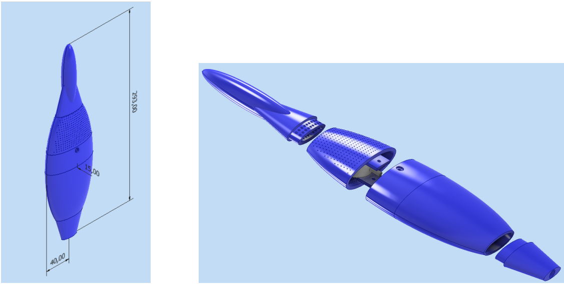

(a) CAD. (b) Exploded view.

Figure 8: Design of the penguin vessel.

The design features four individual pieces that, when assembled, create the vessel. The design features a double eclipse format both in the cross-sectional area and along the direction of the length. The second part has the holes (0.6 mm diameter) through which air is released; it can be observed that the holes are positioned just before the largest cross-sectional area of the design, and near the front. This is so that the bubbles can cover most of the surface while the robot is moving. This part also houses the porous stone, as shown in Figure 8b by the gray component, usually used in aquariums for aeration, which is used for creating very fine bubbles.

4.2. Torpedo shaped vessel

A torpedo-shaped vessel was also designed to compare the effect of bubbles between both systems.The model is shown in Figure 9. The entire design was created using a 3D printer and PETG as the material.

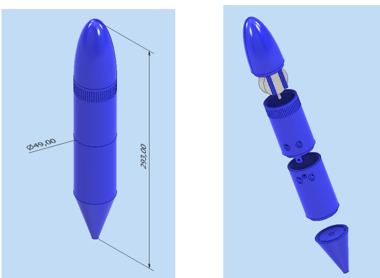

(a) CAD. (b) Exploded view.

Figure 9: Design of the torpedo vessel.

It consists of four parts that are glued together for a tight fit and to avoid any leaking of air during the test. The holes (0.6 mm) are again positioned near the front to cover most of the area of the vessel when moving.

5. Experimental testing

The force measurement was performed using a load cell (CN1501541594). The load cell was connected to an HX711 weight sensor module and an Arduino Uno for measuring the signal, as shown in Figure 10.

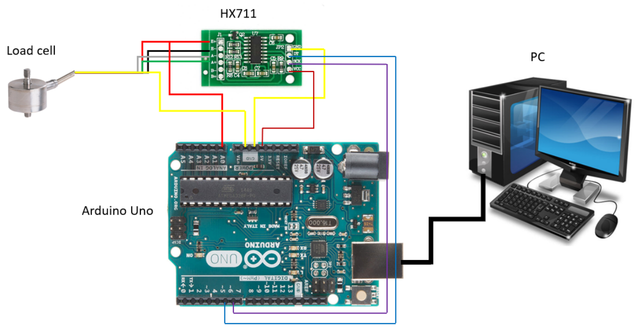

Figure 10: Schematic diagram of the connections of the load cell.

5.1. Code implementation

For the force measurement, a Python code was used to read the signal from the Arduino and automatically make txt files with the data. Then a MATLAB code reads these files, and extracts the force diagram. Then it also calculates the drag coefficient using the vessel's velocity. To calculate the velocity, a checkerboard was placed behind the tank. The checkerboard was a white and red grid of squares that were 2x2 cm. The setup can be seen in the figure below, Figure 11.

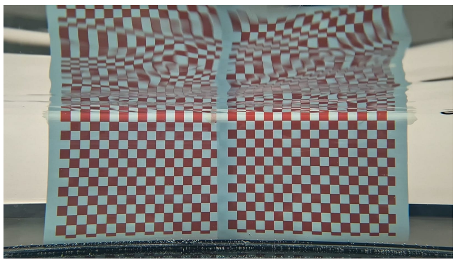

Figure 11: Background setup.

A computer vision code was implemented to measure the speed of the blue vessel that passes through the grid. This MATLAB script is a computer vision program designed to track a blue object (the vessel) and calculate its velocity while correcting for perspective distortion. This is because the object is closer to the camera than the background grid. The script uses the HSV (Hue, Saturation, Value) color space to find the blue vessel. It filters for a specific Hue range (0.55 to 0.75), which corresponds to Blue, and fills in any holes in the object to make it a solid shape. The blue filtering can be seen in Figure 12, the binary mask shows in white what the computer identifies as blue and the rest in black.

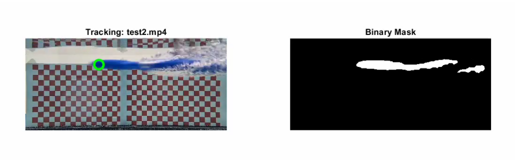

Figure 12: Velocity tracking, the green circle shows the average of the first 100 pixels of the vessel.

Instead of just tracking the center, the code specifically looks for the front edge of the object. Identifies the largest blue blob, sorts the pixels by their X-coordinate, and averages the leftmost pixels. This represents the nose of the vessel. It also uses a weighted average (70% new position, 30% old) to prevent the tracking point from jumping around, Figure 12. Using this position and the calibration with the grid, the code can measure the velocity. The next code focuses on the bubble quantity and dimensions. Using the same calibration as before, the script detects the checkerboard. After the detection is complete, the code remembers the first frame that only shows the checkerboard. Then comes the Image Pre-processing (Isolating Bubbles) part. For this, the script uses three filters to distinguish bubbles from the messy background: HSV Color Filter, Local Contrast Enhancement, which subtracts a blurred version of the image from the original, and Motion Masking, which compares the current frame to the first frame. The filtering can be seen in Figure 13.

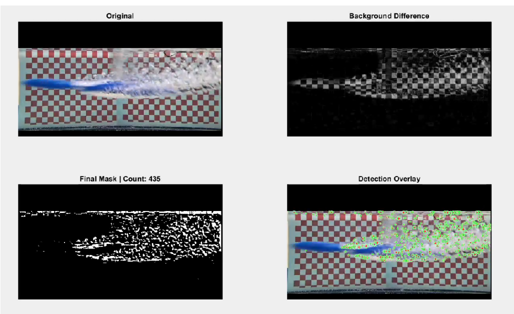

Figure 13: Frame from the display window that is used for bubble tracking.

5.2. Results

Running the tests for both the penguin-inspired robot and the torpedo-inspired robot, after post-processing, we obtain the following results.

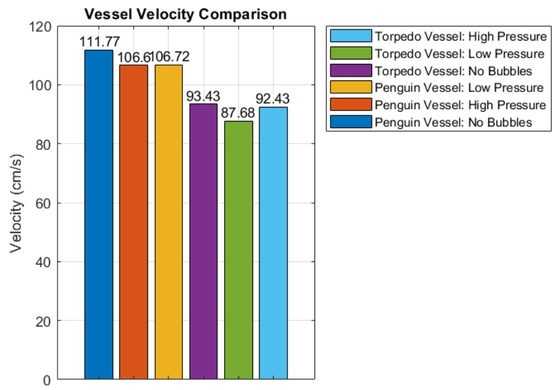

Figure 14: Histogram with the mean velocities from all the tests for both vessels.

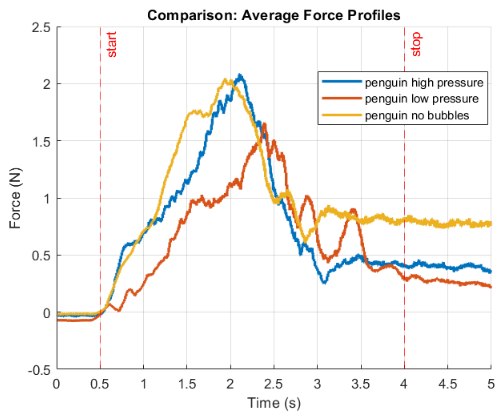

(a)

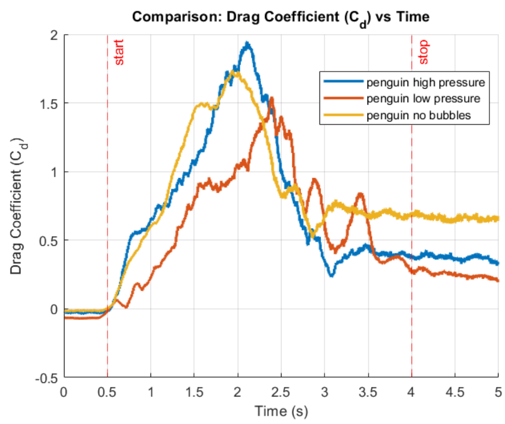

(b)

Figure 15: Graphs of the averaged force (a), and c_d (b) for the penguin.

As it is clearly visible in Figure 15, there is a significant change in the force between the no

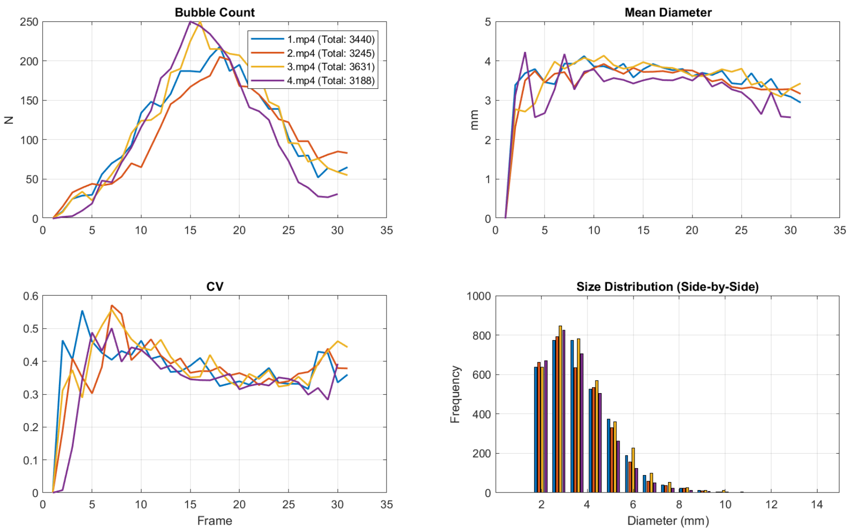

Figure 16: For low pressure (0.5 bar): bubble count, mean diameter, coefficient of variation, and size distribution for the penguin-vessel.

air lubrication test and the low pressure test for the penguin-inspired vessel. The no air bubble test peaks at a value of $\simeq 2.05N$ while the low pressure test peaks at $\simeq 1.66N$, meaning that the bubbles in this pressure (0.5 bar) resulted in a decrease in force of $\simeq 19\%$. Contradictory, increasing the pressure to 1.5 bar did not seem to have a similar effect since the force increased again to $\simeq 2.08N$. Drag coefficient shows a similar trend since the low-pressure c_d, has the lowest peak of $\simeq 1.54$ while the no bubbles has a peak of $\simeq 1.74$, resulting in a $\simeq 11.5\%$ decrease in drag coefficient. Increasing the pressure to 1.5 bar did not reduce the drag coefficient, but increased it, since the force was similar and the velocity for the high-pressure test was lower, resulting in a $\simeq 9.8\%$ increase.

The results for the torpedo did not show anything of particular interest since the bubbles did not reduce the drag. Also, increasing the pressure further increased the drag coefficient. This observation makes the torpedo shape not suitable for drag reduction using the air bubble lubrication method.

During the tests, when the air supply was open, a camera was also capturing the behavior of the bubbles. According to Figure 16, the bubbles produced by the penguin vessel were more in the case of high pressure. Contrary to that, for the torpedo, the low-pressure tests appear to be generating more bubbles, but this is only because the bubbles in the higher pressure are merging too fast into bigger ones before the code can detect them.

6. Conclusions

The final results of drag reduction in a penguin-inspired vessel are quite promising. Drag did reduce for a considerable amount, around 11.5%, with air lubrication. Furthermore, increasing the pressure of the air supply had the opposite effect, increasing the overall drag by around 9.8%. This is due to the bubbles exiting the vessel at a higher speed, resulting in less attachment to the body, as well as increasing the area of the vessel. The torpedo-shaped body also did not show a reduction in drag with air lubrication for both high and low pressure. This might be due to the shape, since the cylinder is not able to hold that many bubbles attached to its underside, like the penguin-shaped body. This is also evident in the bubble detection since the distribution shows very few small bubbles. The speed and bubble detection computer vision algorithms were also quite accurately able to detect the objects. The bubble tracking code, especially, was able to find the difference in bubbles in a very dense bubble cloud when the pressure of the air supply increased.

References

[1] John Davenport, Roger Hughes, Marc Shorten, and Poul S. Larsen. Does drag reduction by air release promote fast ascent in jumping emperor penguins? a novel hypothesis. *Unofficial Draft Version*, December 2008. Unofficial Draft Version (psl) 06-12-2008.

[2] S. H. Marshall, M. W. Chudacek, and D. F. Bagster. A model for bubble formation from an orifice with liquid cross-flow. *Chemical Engineering Science*, 48(11):2049–2059, 1993.

[3] Jie Pan, Ziye Zhou, Jian Wang, Pengfei Zhang, and Junzhi Yu. Development of a penguin-inspired swimming robot with air lubrication system. *IEEE Transactions on Industrial Electronics*, 70(3):2780–2789, March 2023.

[4] Cassondra L. Williams, Julie C. Hagelin, and Gerald L. Kooyman. Hidden keys to survival: the type, density, pattern and functional role of emperor penguin body feathers. *Proceedings of the Royal Society B: Biological Sciences*, 282(1817):20152033, 2015.

[5] Michael J. Wood, Gregory Brock, and Anne-Marie Kietzig. The penguin feather as inspiration for anti-icing surfaces. *Cold Regions Science and Technology*, 213:103903, September 2023.